Computers and Structures 88 (2010) 539–548

Contents lists available at ScienceDirect

Computers and Structures

journal homepage: www.elsevier.com/locate/compstruc

A novel procedure for determination of hydrodynamic pressure along upstream face of dams due to earthquakes

Indrani Gogoi [a,*], Damodar Maity [b]

[a] National Institute of Technology, Surathkal, Karnataka, India
[b] Indian Institute of Technology Kharagpur, India

ARTICLE INFO

Article history:
Received 1 September 2008
Accepted 11 January 2010
Available online 1 February 2010

Keywords:
Earthquake
Hydrodynamic pressure
Infinite reservoir
Truncation boundary
Absorptive reservoir bottom
Short Time Fourier Transform

ABSTRACT

The estimation of hydrodynamic pressures along the upstream face of the dam is a critical parameter for the accurate analysis and design of a dam. The accurate estimation of the hydrodynamic pressures necessitates the consideration of interaction between the dam, the reservoir and the foundation. The interaction effects of the unbounded domain of the reservoir and the absorptive materials deposited at the reservoir bottom are frequency dependent which can be incorporated in a frequency domain procedure easily. But in a time domain procedure the frequency dependent interaction effects are lost. In a frequency domain solution, the excitation frequencies are extracted from the earthquake signal using a Fourier transformation, but do not give any information about how it varies with time. To overcome this, a short-time Fourier transform based formulation is presented in this paper to evaluate the hydrodynamic pressures in time domain to account for the frequency dependent interaction effects of the dam–reservoir system. Thus, the adequate accuracy in the determination of hydrodynamic pressure under earthquake excitation is ensured with the proposed truncation boundary condition.

1. Introduction

The issues of seismic safety of dams have been looked at with increased attention in various parts of the world in recent years. It has become a major factor in the planning and designing of new dams proposed to be built in seismic regions and for safety evaluation of existing dams in these regions. For the design of an earthquake-resistant dam and the evaluation of the safety of an existing dam, it is important to use a rational and reliable dynamic analysis procedure. The dynamic response of a linearly elastic dam can be determined by standard techniques if the reservoir is empty. But the problem becomes complicated, when the interaction effects of the unbounded reservoir and the elastic foundation has to be adequately accounted for. The analysis procedure should be capable of evaluating the dynamic deformations and stresses in a dam subjected to a given ground motion. The deformations and stresses so obtained will be more realistic if the interaction effect of the unbounded reservoir is determined appropriately and the dam–foundation interaction is considered.

For simplification of the analytical procedures, the bottom of the reservoir is generally considered to be rigid, which does not represent the actual behavior of the system. The sedimentary material in the reservoir bottom absorbs or radiates energy at the bottom that will affect the hydrodynamic pressure developed at the upstream face of the dam. An analytical or a closed-form solution cannot account for the arbitrary geometry of the dam or reservoir (Fig. 1). This problem can be efficiently tackled with finite element technique. The need for an accurate truncation boundary is felt to reduce the computational domain of the unbounded reservoir system.

The seismic analysis of dam–reservoir system has intrigued researchers since 1933 [41,39]. The added mass approach was generally used to evaluate the hydrodynamic effects of the reservoir on the dam. Since earthquakes are random in nature, Kotsubo [24] emphasized that evaluation of hydrodynamic pressure using the added mass approach was not accurate. Consequent research carried out by Chopra [7], Chopra and Chakrabarti [9], Saini et al. [32] and Maity and Bhattacharya [28] has shown the importance of considering the compressibility of reservoir water as the hydrodynamic effects of the unbounded reservoir are frequency dependent. Considering the enhanced capabilities of computer processors and increased memory storage, the analysis techniques have improved.

The versatility of the finite element method has motivated researchers to apply the technique in the analysis of dam–reservoir systems. However, while using finite element technique in the analysis of a dam–reservoir system, difficulty arises in effectively modeling the large extent of the reservoir that is practically

* Corresponding author. Tel.: +91 9449046152.
E-mail addresses: indranigogoi@yahoo.com (I. Gogoi), dmaity@civil.iitkgp.ernet.in (D. Maity).

0045-7949/$ - see front matter © 2010 Elsevier Ltd. All rights reserved.
doi:10.1016/j.compstruc.2010.01.007

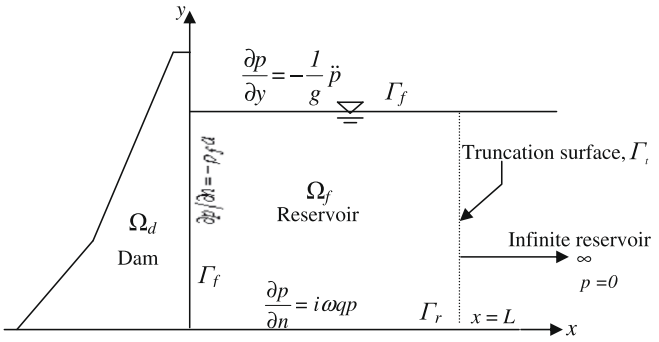

Fig. 1. Reservoir and its boundary conditions.

unbounded. The unbounded reservoir has important consequence in the analysis of the dam–reservoir system, as waves traveling to infinity are not reflected back towards the dam. This leads to the development of an energy dissipation mechanism called radiation damping, which is frequency dependent. The accurate modeling of radiation damping is of extreme importance as it affects the hydrodynamic pressure generated in the reservoir and hence the response of the dam. For efficient numerical solution of the system, the unbounded reservoir is truncated at a certain distance away from the dam. Accuracy in the results may be obtained by truncating the reservoir at a larger distance away from the dam. However, this results in an increased cost of computation. If the effect of dam–reservoir interaction is included in the analysis, the cost of computation will further increase to be prohibitive. Therefore, it is necessary to impose an efficient boundary condition at the truncated surface of the reservoir that can account for radiation damping and reservoir bottom absorption. Various boundary conditions along the truncation surface for the analysis of dam–reservoir system have been developed and used effectively in the frequency domain by Humar and Roufaiel [23], Sharan [34,35] and Li et al. [26]. Although similar boundary conditions have been proposed by Tsai and Lee [36], Maity and Bhattacharyya [28] and Birk and Ruge [2] in the time domain, the boundary conditions do not consider the excitation frequency. The truncation boundary conditions (TBC) using frequency domain approach [34,35] can effectively include the absorption effect of the reservoir bed, which generally cannot be accounted for in time domain approach. The earthquake excitation is generally recorded and used in a time domain solution as a time history, its sensitiveness to the frequency content at every time instant is generally ignored.

The dynamic analysis of a dam–reservoir system can be performed either in time domain or frequency domain. A frequency domain analysis can be adopted when the behavior of the coupled dam–reservoir system is considered to be linear [32,40,5]. Semi-analytical solutions [10] or a combination of finite elements and semi-analytical solution [20,27] may be used for semi-infinite and irregularly shaped reservoirs.

The dynamic performance of a structural system beyond the linear elastic limit cannot be evaluated in the frequency domain using Fourier synthesis as in Chopra and Chakrabarti [9] to obtain solutions due to transient excitations. An effective time domain analysis technique is required for a dynamic nonlinear analysis of a dam–reservoir system. The interaction effects in time domain using a two-dimensional dam–reservoir model were computed by evaluation of convolution integrals [14,37,19] that require considerable computational effort. Darbre [12] and Chavez and Fenves [6] used the hybrid frequency time domain procedure to evaluate the dam–reservoir interaction forces, where the response of the system is computed in frequency domain. The radiation damping in the unbounded reservoir was represented by standard viscous dampers [1,11,25] that need large extent of the reservoir to be considered to obtain an adequate accuracy. Most of the analysis procedures in time domain are too rigorous and complicated; and simplified techniques may not give accurate results. This necessitates an analysis procedure in time domain that can be easily implemented.

For seismic analysis of a dam–reservoir system, the time variation of ground acceleration (a_g) is the most useful way of defining the shaking of the ground during an earthquake. In an accelerogram, the ground motion is defined by numerical values at discrete time instants. Typically the time interval is chosen to be 1/100 to 1/50 of a second [8]. A seismic analysis can be carried out either in the time domain, using time-histories of acceleration or in the frequency domain, calculating frequency content using Fast Fourier Transforms (FFT). The drawback of carrying out a seismic analysis in frequency domain is that when an accelerogram is converted into the frequency domain using an FFT, the time-dependent behavior is lost. In a seismic analysis carried out in time domain, the ground acceleration input is used as a time history and the frequency dependent response of a system can not be determined.

In both soil–structure interaction analyses and fluid–structure interaction, there are phenomena which are frequency dependent, such as radiation damping and reservoir bottom absorption; for which accurate time domain representations are sought. Wolf [42], Wolf and Paronesso [43], Ruge et al. [30], Haigh et al. [22], Safak [31] and Birk and Ruge [2] proposed different techniques to account for the scalar frequency dependent impedance functions into the time domain. The referred literature emphasizes the importance of the need to account for the frequency content of an earthquake excitation, when the dynamic response of the system analyzed is frequency dependent. The Short Time Fourier Transform (STFT) algorithm used by Nagarajaiah and Varadarajan [29] is an effective technique that may be used to determine the time-frequency distribution of an earthquake excitation. The basic idea of STFT is to break up the non-stationary signal into small time segments and obtain the FFT of each time segment to ascertain the frequencies that exist in it.

Since, it is observed that the effect of the boundary conditions imposed at the far end of the reservoir is frequency dependent [17], the hydrodynamic pressure obtained in a time domain solution due to an earthquake may not be sensitive to the frequency content of the earthquake at every time instant. Therefore, in this paper, a unique method of evaluation of hydrodynamic pressure developed on the upstream face of a concrete dam due to seismic excitation is presented. Applying STFT to the time-signal for each time instant, a corresponding frequency is obtained. The coefficient matrices of the time domain model can be calculated in each time step for this frequency. The resulting time domain solution thus takes the frequency content of the transient excitation into account.

2. Time history analysis procedure with frequency dependent boundaries

The present formulation is in time domain, where the dam, the water and the foundation are assumed to have a linear behavior. The reservoir is assumed to have regular rectangular boundaries. The water in the reservoir is considered as non-viscous, linearly compressible and is of small amplitudes of motion. The dam–reservoir–foundation system is treated as two-dimensional. The dam and the reservoir are supported on a flexible foundation modeled as viscoelastic half-plane. The reservoir water is modeled by finite element technique considering pressure as nodal degrees of freedom. The pressure based wave equation may be used to obtain an equation to determine the magnitude of hydrodynamic pres-

sure generated due to small amplitude vibration of compressible but non-viscous water, which can be expressed as

$$\nabla^2 p(x,y,t) = \frac{1}{c^2}\ddot{p}(x,y,t) \tag{1}$$

Here $p(x, y, t)$ is hydrodynamic pressure, t is the time variable, x and y are space variables. The hydrodynamic pressure due to horizontal ground acceleration of rigid dam is the solution of Hemholtz equation (Eq. (1)) subject to the following boundary conditions (Fig. 1). The origin of the horizontal x-axis and vertical y-axis is considered at the bottom of the dam–reservoir interface and accordingly the boundary conditions have been defined.

2.1. At the free surface (Γ_f)

Considering the effects of surface waves of the water, the boundary condition of the free surface [28] is taken as

$$\frac{1}{g}\ddot{p} + \frac{\partial p}{\partial y} = 0 \tag{2a}$$

However, neglecting the effects of surface waves of the water, the boundary condition of the free surface may be expressed as

$$p(x, H_f, t) = 0 \tag{2b}$$

Here, H_f is the depth of the reservoir.

2.2. At the dam–reservoir interface (Γ_{fs})

At the dam–reservoir interface, the pressures should satisfy

$$\frac{\partial p}{\partial n}(0,y,t) = -\rho_f a e^{i\omega t} \tag{3}$$

where $ae^{i\omega t}$ is the horizontal component of the ground acceleration in which, ω is the circular frequency of vibration and $i = \sqrt{-1}$, n is the outwardly directed normal to the elemental surface along the interface. ρ_f is the density of the reservoir water.

2.3. At the reservoir bed interface (Γ_r)

The absorption of pressure waves at the bottom of the reservoir is modeled by using the technique proposed by Hall and Chopra [20]. Thus the condition may be expressed as:

$$\frac{\partial p}{\partial n}(x,0,t) = -\rho_f a_n(t) - q\dot{p}(x,0,t) \tag{4}$$

Assuming a time harmonic behavior of pressure $p(x,0,t) = p(x,0,t)e^{i\omega t}$, the above equation may also be expressed as

$$\frac{\partial p}{\partial n}(x,0,t) = -\rho_f a_n(t) + i\omega q p(x,0,t) \tag{5}$$

Here, n is the outwardly directed normal to the elemental surface along the interface and the coefficient

$$q = \frac{1}{c}\left(\frac{1-\alpha}{1+\alpha}\right) \tag{6}$$

The frequency independent reflection coefficient, α is given as

$$\alpha = \frac{1 - \frac{\rho c}{\rho_s c_s}}{1 + \frac{\rho c}{\rho_s c_s}} \tag{7}$$

Here, ρ_s is the mass density of sediment, $c_s = \sqrt{E_s/\rho_s}$ is the compression wave velocity in the reservoir bed, where E_s = elastic modulus of the sediment.

2.4. At the truncation boundary (Γ_t)

The specification of the far-boundary condition is one of the most important features in the FE analysis of a semi-infinite or infinite reservoir. This is due to the fact that the developed hydrodynamic pressure, which affects the response of the structure, is dependent on the truncation boundary condition. Application of Sommerfeld radiation condition [44] at the truncation boundary leads to

$$\frac{\partial p}{\partial x}(L,y,t) = 0 \tag{8}$$

L represents the distance between the structure and the truncation boundary. Incorporating the effect of reservoir bottom absorption, Sharan [35] has incorporated the following condition

$$\frac{\partial p}{\partial x}(L,y,t) = -\frac{\zeta}{H}p(L,y,t) \tag{9}$$

Here, ζ is a complex damping parameter imposed at the truncation boundary. The main drawback of the above condition is that it is non-local and does not produce reasonably accurate results at second and third eigen frequencies [33].

The proposed condition along the truncation boundary for the compressible fluid domain is derived from the wave equation. The general solution of Eq. (1) satisfying Eqs. (2)–(4) and the radiation condition, can be solved by the method of separation of variables [3] to obtain the hydrodynamic pressure $p(x, y, t)$ at any point (x, y) at a time instant t can be given,

$$p(x,y,t) = -2\rho a H_f \sum_{m=1}^{\infty} \frac{\lambda_m^2 I_m}{\beta_m k_m} e^{(-k_m x)}(\Psi_m)e^{i\omega t} \tag{10}$$

where a is the applied acceleration at the fluid–structure interface in the normal direction and

$$I_m = \frac{1}{H_f}\int_0^{H_f} \Psi_m \, dy \tag{11}$$

$$\Psi_m = \frac{1}{2\lambda_m}\left[(\lambda_m + \omega q)e^{i\lambda_m y} + (\lambda_m - \omega q)e^{-i\lambda_m y}\right] \tag{12}$$

$$\lambda_m^2 = \left(\frac{(2m-1)\pi}{2H_f}\right)^2 + i2\omega q/H_f \tag{13}$$

$$k_m = \sqrt{\lambda_m^2 - \Omega'^2} \tag{14}$$

$$\beta_m = (\lambda_m^2 - \omega^2 q^2)\left(H - \frac{\chi}{\lambda_m^2 + \chi^2}\right) + i\omega q \tag{15}$$

$$\Omega' = \omega/c \tag{16}$$

$$\chi = \frac{\omega^2}{g} \tag{17}$$

The value of χ can be considered to be zero if the effect of gravity waves is neglected. For a rigid reservoir bottom, $q = 0.0$ and $\alpha = 1.0$, for which the pressure obtained is real valued. Generally, determination of the eigenvalues λ_m requires use of advanced programming techniques such as Newton-Raphson method implemented in specialized finite element program like Earthquake Analysis of Concrete Gravity Dams, EAGD [15]. Here, a simplified technique as proposed by Bouaanani et al. [4] is used to determine the eigenvalues. To obtain a finite model of the infinite reservoir, a truncation boundary proposed by Gogoi and Maity [17] is imposed on the truncation surface as:

$$\frac{\partial p}{\partial n} = \left(\zeta_m - \frac{1}{c}\right)\dot{p} \tag{18}$$

where ζ_m is obtained as follows:

$$\zeta_m = -\frac{i\sum_{m=1}^{\infty}\frac{\lambda_m^2 I_m}{\beta_m}e^{(-k_m x)}(\Psi_m)}{\Omega' c\sum_{m=1}^{\infty}\frac{\lambda_m^2 I_m}{\beta_m k_m}e^{(-k_m x)}(\Psi_m)} \tag{19}$$

The effect of reservoir bottom absorption is an important parameter that influences the response of a dam–reservoir system during an earthquake. The dynamic problem of a dam–reservoir system has been rigorously analyzed in the frequency domain considering the effects of radiation damping and reservoir bottom absorption [20,35,21]. Many time domain models consider radiation damping with standard viscous dampers [38,13,37]. The reservoir bottom absorption effect is frequency dependent, which makes it difficult to incorporate in a time history analysis as the solution procedure cannot account for the frequency content of the seismic excitation at every time instant. In an endeavor to understand the behavior of structural systems due to earthquake excitation various techniques are being developed to account for the frequency dependent parameters [22,31] in a time history analysis. It is evident from Eqs. (4) and (18) that boundary conditions at the reservoir bottom and truncation surface respectively are sensitive to excitation frequency. Hence, it is important to estimate the frequency content of an earthquake signal at every time step to effectively account for radiation damping and reservoir bottom absorption effect.

A Fourier transformation generally breaks down a signal into constituent sinusoids of different frequencies. While transforming a time-based signal to frequency domain, the time information is lost and it is difficult to obtain the frequency information at a particular time instant. To overcome this deficiency, Gabor [16] adapted the Fourier transform to analyze only a small section of the signal at a time – a technique called *windowing* the signal. Gabor's adaptation, called the *Short-Time Fourier Transform* (STFT), maps a signal into a two-dimensional function of time and frequency. However, the information obtained by STFT has limited precision, and that precision is determined by the size of the window.

Here, the technique commonly used in digital signal processing called Short Time Fourier Transformation (STFT) has been adopted to determine the frequencies at a time instant. To capture the time variation of the frequency contents of the signal, the signal $S(\tau)$ is multiplied by a sliding window $h(\tau - t)$, centered at time t, and taking the Fourier transform of the weighted signal. Mathematically,

$$S_t(\omega) = \int_{-\infty}^{+\infty} S(\tau)h(\tau - t)e^{-i\omega\tau}\,d\tau \tag{20}$$

gives the Short Time Fourier Transform at every window. The spectral density of the modified signal at every time instant, t can be obtained by

$$P(t,\omega) = |S_t(\omega)|^2 \tag{21}$$

The instantaneous frequency at time t can be located from the center of the $S_t(\omega)$ by taking its first moment as

$$\omega_t = \frac{\int \omega|S_t(\omega)|^2\,d\omega}{\int |S_t(\omega)|^2\,d\omega} \tag{22}$$

The hydrodynamic pressure $p(x, y, t)$ can be determined accurately at every instant of time by incorporating the instantaneous excitation frequency of the earthquake signal obtained by Eq. (22) in the boundary conditions at the reservoir–reservoir bed interface and truncation boundary defined by Eqs. (4) and (18) respectively. The finite element implementation for determination of hydrodynamic pressure due to horizontal ground acceleration is given in Appendix A. The frequency dependent coefficient matrices [A] and [G] as in Eq. (A-15) have different values in each time step. They are calculated in each time step using the frequency corresponding to this time step obtained using the STFT of the earthquake excitation. [A] and [G] are thus time-dependent, but piece-wise constant (constant within one time step). In this case, a standard algorithm for the numerical solution of (A-14) is used, with different values of [A] and [G] in each time step.

3. Seismic analysis of dam–reservoir system using Short Time Fourier Transform

The present boundary conditions at the reservoir bottom and the truncated surface are frequency dependent (Eqs. (5) and (18)). Therefore, to increase the efficiency and accuracy of present algorithm for seismic analysis in time domain, the spectral content of the seismic excitation is extracted and incorporated in the present analysis as explained.

3.1. Extraction of frequencies from time history data of recorded earthquake

The earthquake data represented by accelerograms as shown in Figs. 2 and 3 do not indicate the frequency components of the earthquake signal. A Fast Fourier Transform (FFT) converts the signal to frequency domain and can be used to obtain the power spectrum, which is a measurement of power at various frequencies (Fig. 4). The ground accelerations due to El Centro earthquake (1940) is recorded at a time step of $\Delta t = 0.02$. Therefore, this set of data is sampled at frequency, $f_n = 1/\Delta t$, i.e., 50 Hz. The accelerations due to Koyna earthquake (1967) are recorded at a time step, $\Delta t = 0.01$. Hence, this set of data is sampled at a frequency, $f_n = 100$ Hz. A FFT of El Centro earthquake gives its power spectrum (Fig. 4) that shows the variation of energy with frequencies. A normalized discrete-time Fourier transform can be obtained as $P_n = \text{abs}\,(\text{FFT}(\boldsymbol{S})) \times 2/\text{length}(\boldsymbol{S})$ and is plotted in Fig. 5. Here $\boldsymbol{S}$ represents the earthquake excitation in time domain. It is apparent from these figures that the amplitude of the earthquake excitation is not significant at higher frequencies.

The Short Time Fourier Transform (STFT) of the El Centro earthquake signal is evaluated at $\Delta t = 0.02$ s (Fig. 6) and at $\Delta t = 0.002$ s (Fig. 7). The frequency inputs in the proposed algorithm at each time step are the frequencies corresponding to the maximum spectral density in the moving window. These dominant frequencies are adopted as excitation frequency at each time step. When the time step is large ($\Delta t = 0.02$ s), the number of samples per window is less than when the signal is sampled at $\Delta t = 0.002$ s. It is observed from the figures that a larger time sampling may lead to inaccuracy in frequency evaluation, as it may not be possible to extract all the important frequencies present in the signal. The width of the windowing function determines whether the frequency resolution or the time resolution is good. A wide window, i.e., a large

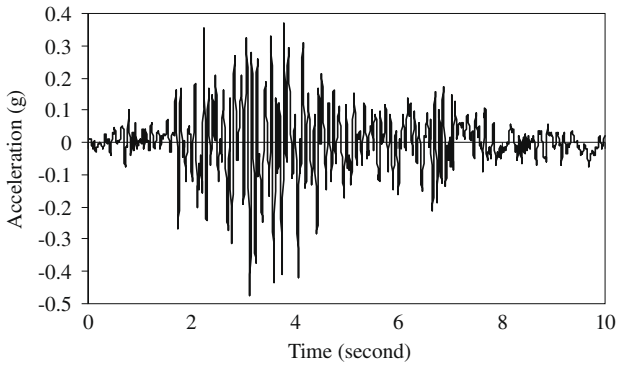

Fig. 2. Horizontal accelerogram of Koyna earthquake, December 11, 1967.

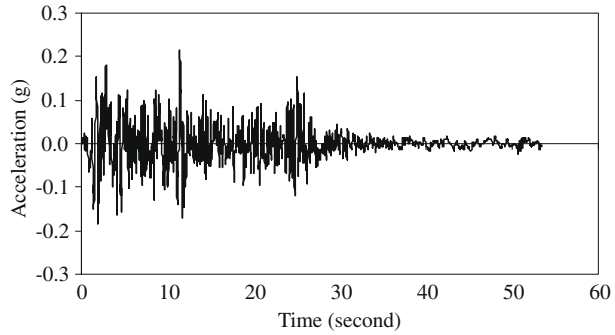

Fig. 3. East–West Component of El Centro earthquake of May 18, 1940.

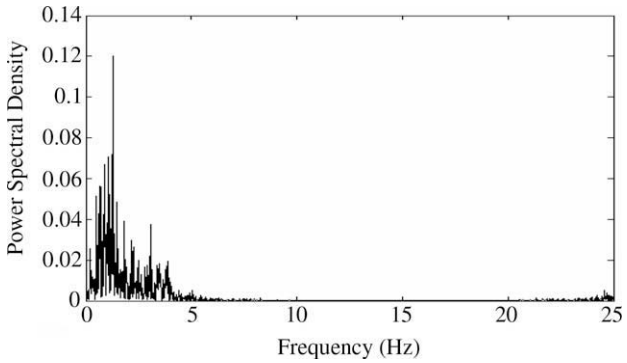

Fig. 4. Power spectrum of East–West Component of El Centro earthquake.

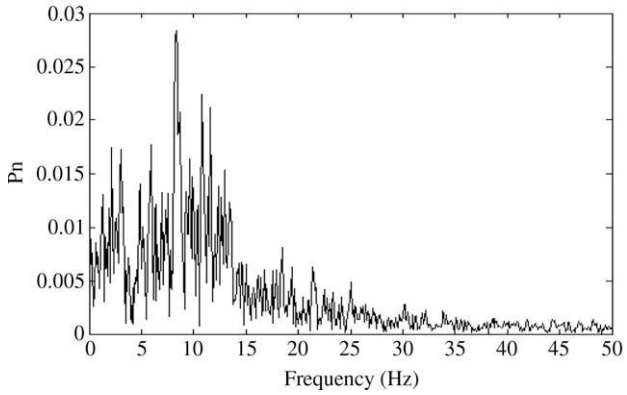

Fig. 5. Normalised FFT of the horizontal component of Koyna earthquake, 1967.

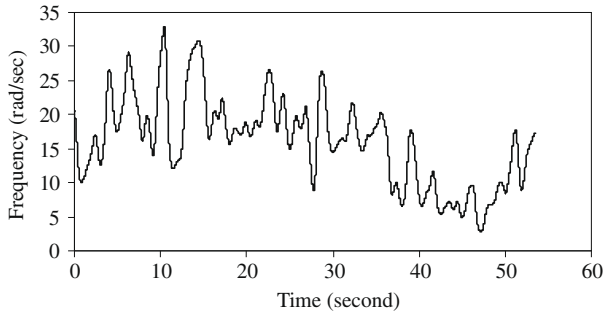

Fig. 6. STFT of El Centro earthquake, 1940 ($\Delta t = 0.02$ s).

time step gives better frequency resolution but poor time resolution. A narrower window, i.e., a small time step gives good time

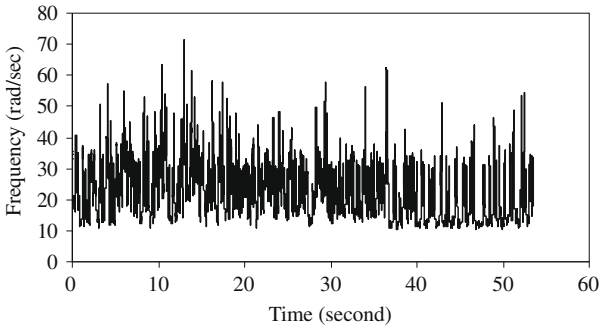

Fig. 7. STFT of El Centro earthquake, 1940 ($\Delta t = 0.002$ s).

resolution but poor frequency resolution. It is seen that the peak frequency is less than 35 rad/s when sampled at $\Delta t = 0.02$ s (Fig. 6), whereas the peak frequency reaches 70 rad/s when sampled at $\Delta t = 0.002$ s (Fig. 7). Considering a very small time step such as $\Delta t = 0.001$ may reflect inaccurate frequency. Fig. 8 shows the STFT of the Koyna earthquake (Fig. 2) sampled at $\Delta t = 0.005$ s, where the frequencies of the Koyna earthquake reach a peak value of 80 rad/s. However, the time step selected should be same as that adopted by a convergence study for the solution of hydrodynamic pressure using Eq. (A-14) [18].

3.2. Hydrodynamic pressure neglecting dam flexibility due to seismic excitation

The hydrodynamic pressure developed at the bottom of the dam–reservoir interface due to seismic excitation is evaluated. Here, the upstream face of the dam is considered to be vertical and bottom of the reservoir to be horizontal. Due to lack of analytical technique to evaluate the hydrodynamic response of the reservoir due to seismic excitation, the accuracy of the proposed technique is verified by convergence study. The effectiveness of the proposed boundary condition using Short Time Fourier Transform (STFT) is examined for different reservoir depths and earthquake excitations. The hydrodynamic pressure coefficient is evaluated for a reservoir depth of (i) 30 m and (ii) 150 m considering the frequency content of East–West Component of El Centro earthquake (1940). At a reservoir depth of 30 m, the fundamental frequency of the reservoir is 75.398 rad/s, which is higher than the peak frequency content of the earthquake excitation (approximately 70 rad/s as seen in Fig. 7). At a reservoir depth of 150 m, the fundamental frequency of reservoir becomes 15.07 rad/s which is less than the peak frequency content of the earthquake excitation. A convergence study was carried out by Gogoi and Maity [17] to study the effectiveness of the present boundary condition. It was observed from the results that a reservoir length of $L = 0.5H_f$ is effective for all ranges of excitation frequencies to determine the

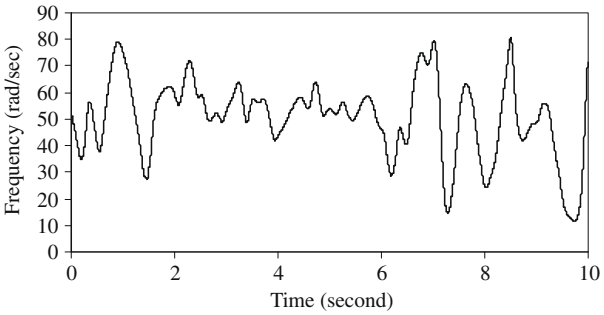

Fig. 8. STFT of Koyna earthquake, 1967 ($\Delta t = 0.005$ s).

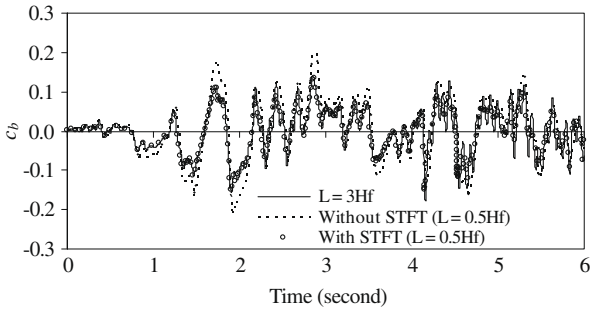

Fig. 9. Hydrodynamic pressure coefficient at the bottom of dam–reservoir interface due El Centro earthquake (H_f = 30 m).

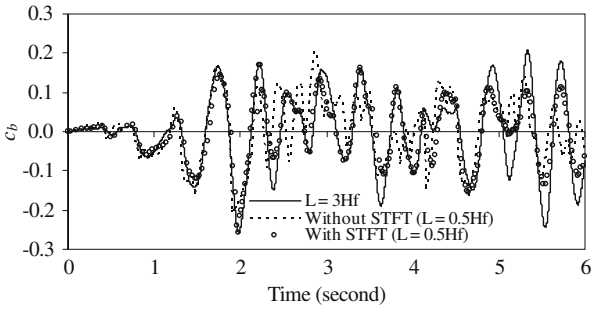

Fig. 10. Hydrodynamic pressure coefficient at the bottom of dam–reservoir interface due El Centro earthquake (H_f = 150 m).

hydrodynamic pressure in the reservoir due to harmonic excitation. Therefore, the hydrodynamic pressure coefficients, are evaluated at the vertical upstream face of the dam considering a length of the reservoir, $L = 0.5H_f$ for the first 6 s and compared with that obtained at $L = 3.0H_f$, which is considered to be the exact result as a large fluid domain is included in the analysis. Here, the hydrodynamic pressure coefficient is given by $c_b = p_b/\rho_f a H_f$, where p_b is the maximum hydrodynamic pressure at the base of the upstream face of the dam. The reflection coefficient is considered as 0.5 for the seismic analysis. It is interesting to note from Figs. 9 and 10 that consideration of STFT in the seismic analysis increases the effectiveness of the proposed truncation boundary condition.

The hydrodynamic pressure coefficients are determined for the reservoir having the same parameters as in the previous case considering the Koyna earthquake. It is seen from the Figs. 11 and 12, that the hydrodynamic response due to Koyna earthquake can be obtained accurately by imposing the proposed truncation boundary at a distance of $L = 0.5H_f$. This is because the fundamental frequencies of the reservoir having depth of 30 m and 150 m are less than the peak frequency content of Koyna earthquake, which is approximately 80 rad/s. It is observed from the results (Figs. 13 and 14) that effectiveness of the proposed algorithm in determining the hydrodynamic pressures is improved with the use of STFT. When the STFT of the earthquake is not considered the effect of frequency dependent absorption at the reservoir can not be effectively accounted for, which as a result gives higher magnitudes of hydrodynamic response.

The hydrodynamic pressure distribution developed due to seismic excitation (Koyna earthquake, 1967) along the dam–reservoir interface is further studied for different depths of sediment layer. The depth of the reservoir (H_f) is considered to be 150 m. The depth

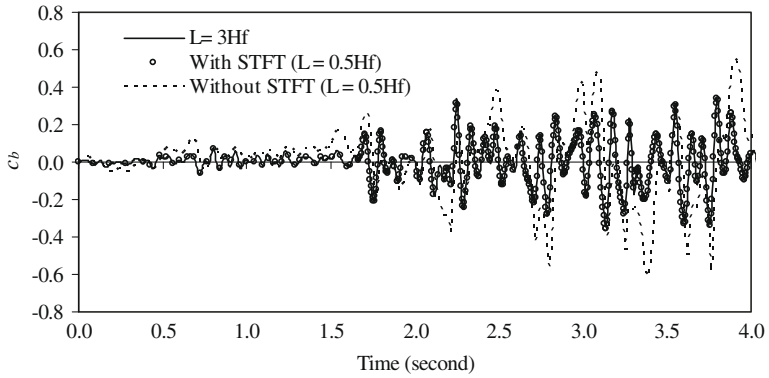

Fig. 11. Maximum hydrodynamic pressure coefficient at the bottom of dam–reservoir interface due to Koyna earthquake (H_f = 30 m).

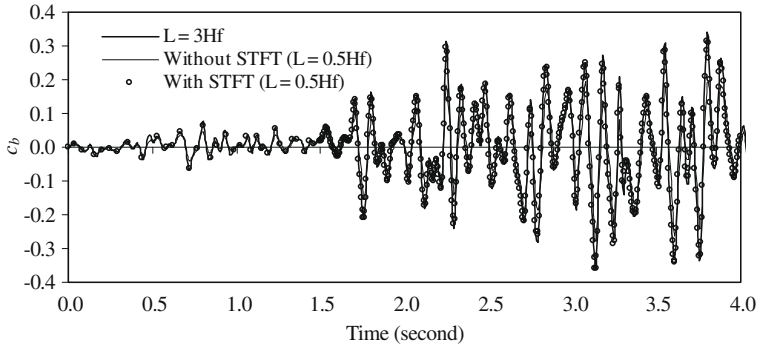

Fig. 12. Maximum hydrodynamic pressure coefficient at the bottom of dam–reservoir interface due to Koyna earthquake (H_f = 150 m).

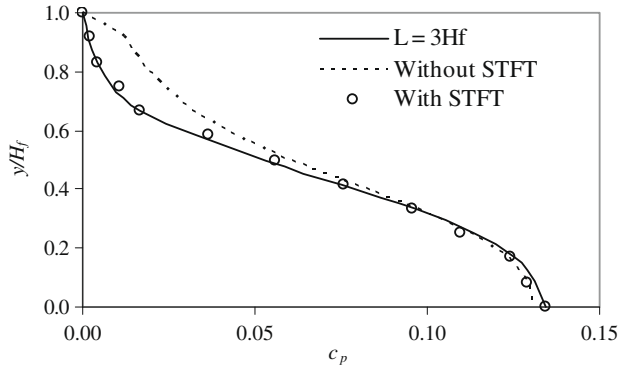

Fig. 13. Hydrodynamic pressure distribution along dam–reservoir interface due to seismic excitation at $t = 2.94$ s ($d_s = 0.01H_f$).

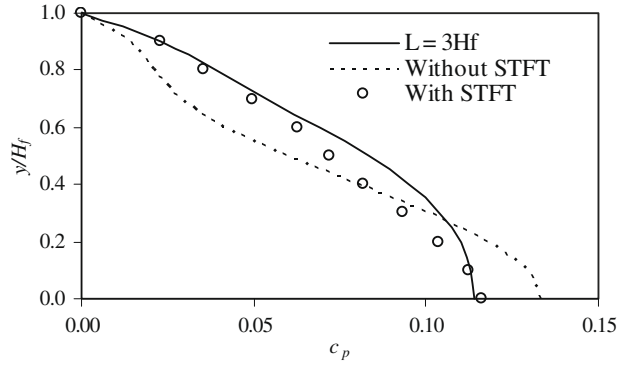

Fig. 14. Hydrodynamic pressure distribution along dam–reservoir interface due to seismic excitation, at $t = 2.94$ s ($d_s = 0.1H_f$).

of sediment layer (d_s) is expressed in terms of the reservoir depth (H_f). The infinite domain of the reservoir is truncated at $L = 0.5H_f$. It is observed from Fig. 15 that the effect of increase in sediment layer depth is significant until $d_s = 0.1H_f$, beyond which an increase in sediment depth to $d_s = 0.5H_f$ has no effect on the hydrodynamic pressure developed.

3.3. Hydrodynamic pressure considering dam–reservoir interaction due to seismic excitation

To evaluate the effectiveness of the developed truncation boundary condition (TBC) with the incorporation of Short Time Fourier Transform (STFT) in the proposed algorithm for dam–reservoir interaction, a typical dam–reservoir system is considered having geometry as shown in Fig. 16. The dimension and the material properties of the dam in the present case are: height of the dam = 103 m; width at the top of the dam is 14.8 m and at the base is 70.0 m, modulus of elasticity = 31,500 MPa; Poisson's ratio = 0.235 and mass density = 2415.816 kg/m^3. Structural damping is considered as 3%. The dam is discretized with 8-noded quadratic elements and is analyzed using plain strain formulation. In the present investigation, the dynamic magnifications of strength and stiffness parameters due to rapid application of seismic strains are not considered. The depth of the water is considered to be equal to the height of the dam. The acoustic wave speed in water and the mass density of water are considered to be 1438.7 m/s and 999.8 kg/m^3 respectively. Due to lack of classical solution, the response of the coupled dam–reservoir system is compared with those obtained at $L = 3.0H_f$. The crest displacement of the dam and the hydrodynamic pressure coefficient (c_b) at the bottom of the upstream face of the dam due to the horizontal component of Koyna earthquake are presented herein. It is evident from Figs. 17 and 18 that at $L = 0.5H_f$, the algorithms using STFT gives crest displacements and pressure coefficients without much loss in accuracy.

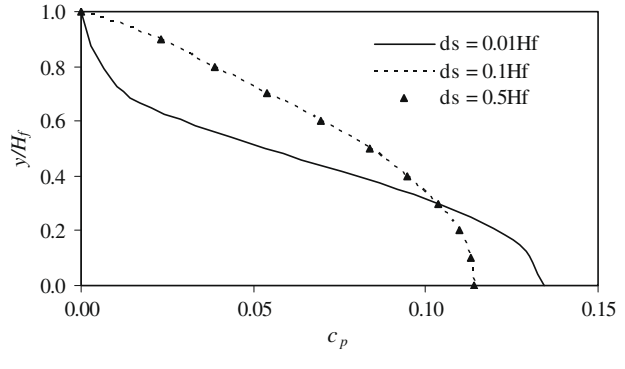

Fig. 15. Effect of sediment layer thickness on hydrodynamic pressure distribution along dam–reservoir interface due to seismic excitation at $t = 2.94$ s.

The random vibration caused by an earthquake generally consists of many frequencies. Hence, it is important to evaluate the effectiveness of the proposed algorithm for seismic analysis of dam–reservoir system in time domain. To observe the effect of the reservoir bottom absorption due to seismic excitation, the dam with the same material and geometrical properties as above is considered. The variation of normalized crest displacement due to Koyna earthquake (Fig. 2) is plotted to observe the effect of absorption at the reservoir bottom. It is observed from Figs. 19 and 20 that the crest displacement and hydrodynamic pressure coefficient (c_b) is reduced considerably due to absorptive reservoir

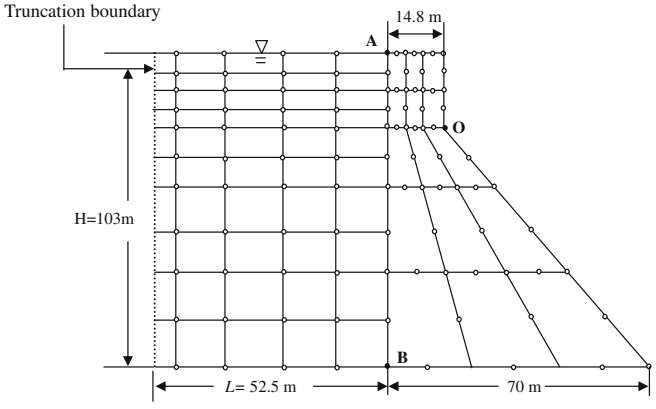

Fig. 16. Finite element mesh of dam–reservoir system.

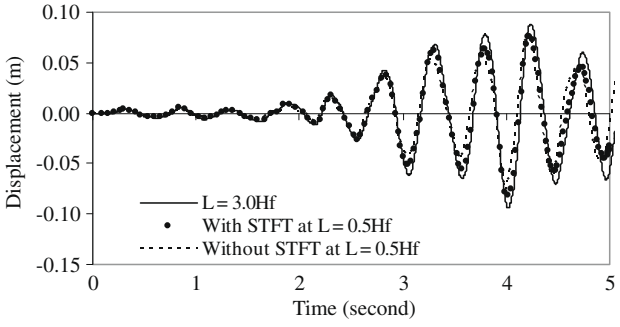

Fig. 17. Crest displacement of dam due to Koyna earthquake.

bottom with reflection coefficient of $\alpha = 0.5$. The hydrodynamic pressure at the upstream face of the dam depends on the acceleration of the dam–reservoir interface. The acceleration of the flexible dam thus affects the hydrodynamic response due to seismic excitation.

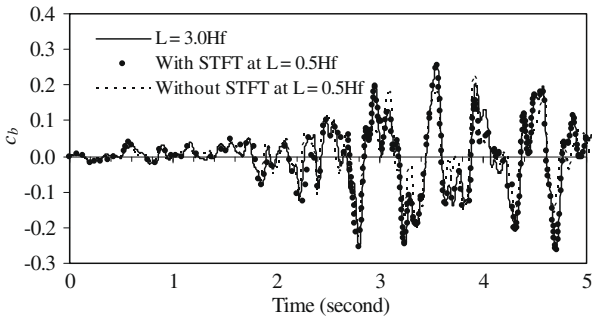

Fig. 18. Hydrodynamic pressure at the bottom of the dam due to Koyna earthquake.

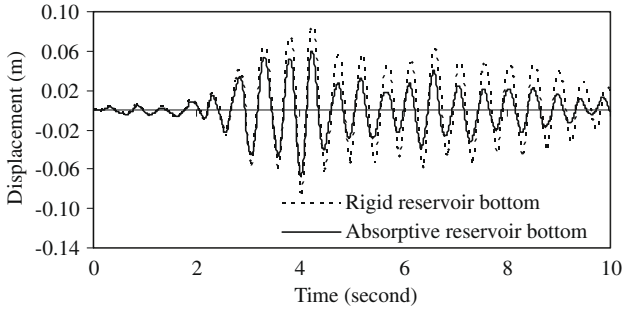

Fig. 19. Effect of reservoir bottom absorption on crest displacement of the dam due to Koyna earthquake.

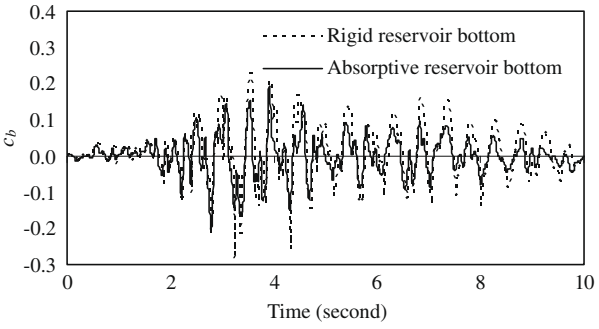

Fig. 20. Effect of reservoir bottom absorption on hydrodynamic pressure coefficient at point B due to Koyna earthquake.

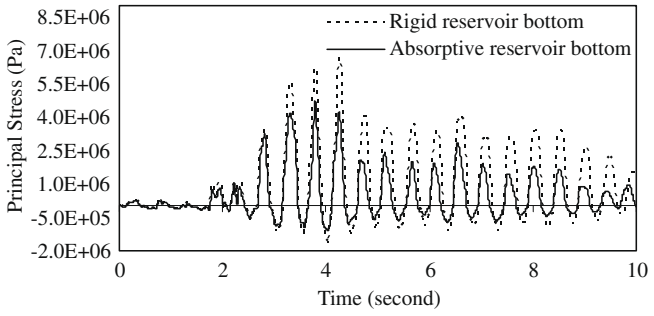

Fig. 21. Effect of reflection coefficient on principal stress σ_{p1} at point B of the dam due to Koyna earthquake.

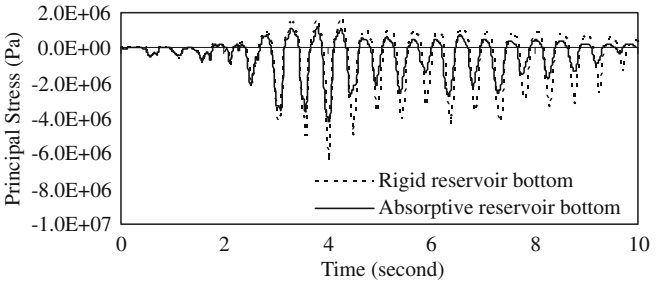

Fig. 22. Effect of reflection coefficient on principal stress σ_{p2} at point B of the dam due to Koyna earthquake.

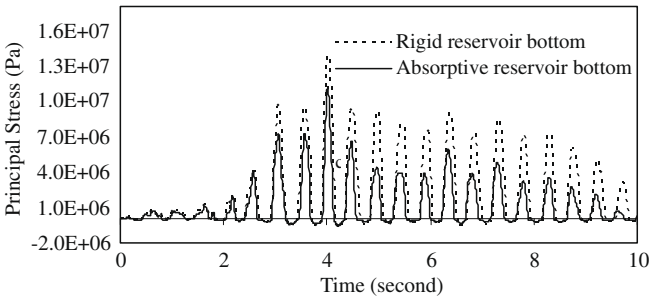

Fig. 23. Effect of reflection coefficient on principal stress σ_{p1} at point O of the dam due to Koyna earthquake.

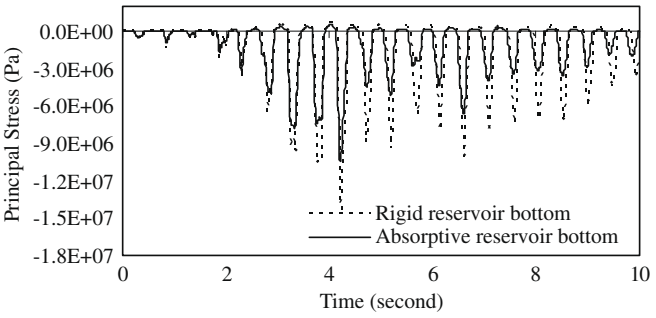

Fig. 24. Effect of reflection coefficient on principal stress σ_{p2} at point O of the dam due to Koyna earthquake.

The principal stresses σ_{p1} (maximum tensile and minimum compressive) and σ_{p2} (maximum compressive and minimum tensile) at point B and O (Fig. 16) are plotted in Figs. 21–24 respectively. It is observed from these graphs that the principal stresses in the dam reduce significantly in the presence of the absorptive reservoir bottom. It is interesting to note that the magnitudes of stresses at the point O are higher than the stresses at point B because of development of stress concentration.

4. Conclusions

A novel procedure of seismic analysis in the time domain analysis is presented in this paper that accounts for the frequency dependent boundary conditions at the reservoir bottom and truncation surface. The algorithm proposed considers the frequency content of earthquake excitation so that the damping parameters at the reservoir bottom and truncation surface can be estimated accurately. The non-stationary earthquake signal is divided into

small time segments and the FFT of each time segment is obtained to ascertain the frequencies that exist in it. The dominant frequency at every time step is extracted and is used as an input in the seismic analysis. The effectiveness of the developed far-boundary condition has been increased with the incorporation of Short Time Fourier Transform (STFT) for the analysis of dam–reservoir system under seismic excitation. The proposed time-frequency hybrid method is advantageous as the frequency dependent responses of the dam–reservoir system can be obtained in a time domain procedure. The implementation of this technique is simple as the time domain procedure remains the same and the algorithm can be modified to account for the dominant frequencies at every time step. As the procedure is in time domain and can efficiently account for different excitation frequencies the transformation of frequency dependent dynamic stiffness matrix as used in various time-frequency hybrid methods can be avoided.

Appendix A

A.1. Finite element implementation for determination of hydrodynamic pressure due to horizontal ground acceleration

By the use of Galerkin process, and assuming pressure to be the nodal unknown the discretized form of Eq. (1) may be written in two-dimension as

$$\int_{\Omega} N_{rj}\left[\nabla^2 \sum N_{ri} p_i - \frac{1}{c^2}\sum N_{ri}\ddot{p}_i\right] d\Omega = 0 \tag{A-1}$$

where N_{rj} is the interpolation function for the reservoir and Ω is the region under consideration. Using Green's theorem Eq. (A-1) may be transformed to

$$-\int_{\Omega}\left[\frac{\partial N_{rj}}{\partial x}\sum \frac{\partial N_{ri}}{\partial x} p_i + \frac{\partial N_{rj}}{\partial y}\sum \frac{\partial N_{ri}}{\partial y} p_i\right] d\Omega - \frac{1}{c^2}\int_{\Omega} N_{rj}\sum N_{ri}\, d\Omega \ddot{p}_i + \int_{\Gamma} N_{rj}\sum \frac{\partial N_{rj}}{\partial n} d\Gamma p_i = 0 \tag{A-2}$$

in which i varies from 1 to total number of nodes and Γ represents the boundaries of the fluid domain. The last term of the above equation may be written as

$$\{B\} = \int_{\Gamma} N_{rj}\frac{\partial p}{\partial n} d\Gamma \tag{A-3}$$

The whole system of Eq. (A-2) may be written in a matrix form as

$$[\overline{H}]\{\ddot{p}\} + [\overline{G}]\{p\} = \{B\} \tag{A-4}$$

in which,

$$\left.\begin{aligned} [\overline{H}] &= \tfrac{1}{c^2}\textstyle\sum \int_{\Omega}[N_r]^T[N_r]d\Omega \\ [\overline{G}] &= \textstyle\sum \int_{\Omega}\left[\frac{\partial}{\partial x}[N_r]^T\frac{\partial}{\partial x}[N_r] + \frac{\partial}{\partial y}[N_r]^T\frac{\partial}{\partial y}[N_r]\right]d\Omega \\ \{B\} &= \textstyle\sum \int_{\Gamma}[N_r]^T\frac{\partial p}{\partial n}d\Gamma = \{B_f\} + \{B_{fs}\} + \{B_r\} + \{B_t\} \end{aligned}\right\} \tag{A-5}$$

Here the subscript f, fs, r and t stand for the free surface, fluid–structure interface, reservoir bottom–fluid interface and truncation surface respectively. According to the boundary conditions for the fluid domain, if linearised surface wave condition is adopted (Eq. (2)), the same may be written in finite element form as

$$\{B_f\} = -\frac{1}{g}[R_f]\{\ddot{p}\} \tag{A-6}$$

in which,

$$[R_f] = \sum \int_{\Gamma_f}[N_r]^T[N_r]d\Gamma \tag{A-7}$$

At the dam–reservoir interface (Eq. (3)), if $\{a\}$ is the vector of nodal accelerations of generalized coordinates, $\{B_{fs}\}$ may be expressed as

$$\{B_{fs}\} = -\rho_f[R_{fs}]\{a\} \tag{A-8}$$

where,

$$[R_{fs}] = \sum \int_{\Gamma_{fs}}[N_r]^T[T][N_d]d\Gamma \tag{A-9}$$

Here, $[T]$ is the transformation matrix for generalized accelerations of a point on the fluid–structure interface and $[N_d]$ is the matrix of shape functions of the dam used to interpolate the generalized acceleration at any point on the fluid–structure interface in terms of generalized nodal accelerations of an element. At the reservoir bed (Eq. (5)), $\{B_r\}$ may be expressed as

$$\{B_r\} = i\omega q[R_r]\{p\} - \rho_f[R_r]\{a'\} \tag{A-10}$$

where,

$$[R_r] = \sum \int_{\Gamma_r}[N_r]^T[N_r]d\Gamma \tag{A-11}$$

From the condition specified by Eq. (18) at the truncation boundary, the following expression emerges.

$$\{B_t\} = \left(\zeta_m - \frac{1}{c}\right)[R_t]\{\dot{p}\} \tag{A-12}$$

where,

$$[R_t] = \sum \int_{\Gamma_t}[N_r]^T[N_r]d\Gamma \tag{A-13}$$

Substitution of all terms in Eq. (A-4) gives

$$[H]\ddot{p}\} + [A]\{\dot{p}\} + [G]\{p\} = \{F_r\} \tag{A-14}$$

Here, $[H]$, $[A]$, $[G]$ and $\{F_r\}$ can be expressed as

$$\left.\begin{aligned} [H] &= [\overline{H}] + \tfrac{1}{g}[R_f] \\ [A] &= (\tfrac{1}{c} - \zeta_m)[R_t] \\ [G] &= [\overline{G}] - i\omega q[R_r] \\ \{F_r\} &= -\rho_f([R_{fs}]\{a\} + [R_r]\{a'\}) \end{aligned}\right\} \tag{A-15}$$

For any prescribed acceleration at the dam–reservoir interface and reservoir bed interface, Eq. (A-14) is solved to obtain the hydrodynamic pressure in the reservoir.

Appendix B

B.1. Theoretical formulation for dam–reservoir system

In the dam–reservoir interaction problems, the dam and the reservoir do not vibrate as separate systems under external excitations, rather they act together in a coupled way. Therefore, these problems have to be dealt in a coupled way. An iterative scheme is developed in the present study to achieve the coupled effect of dam–reservoir system.

Initially, the dam is assumed to be rigid. The resulting hydrodynamic pressure is evaluated by solving the reservoir domain using Eq. (A-10) with appropriate boundary conditions at any instant of time t. However, since the objective is to achieve a solution for an elastic dam–reservoir interaction, the resulting pressure is inaccurate. The developed pressures exert forces $\{F_r\}$ on the adjacent dam. Hence, at the same time instant, the concrete dam is analyzed with the forces $\{F_r\}$, developed due to hydrodynamic pressures at the dam–reservoir interface, using the equation

$$[M]\{\ddot{d}\} + [C]\{\dot{d}\} + [K]\{d\} = \{F_d\} + \{F_r\} \tag{B-1}$$

where $\{F_d\} = -[M]a_g$. Due to these additional forces $\{F_r\}$, the dam undergoes a displacement $\{d\}_t$. As a result the dam–reservoir interface boundary changes and hence the solution of the reservoir domain. The reservoir domain is solved again at the same time instant with the changed conditions of displaced structural boundary. Consequently the structural system is also analyzed with the changed forces. Thus at time t, both the hydrodynamic pressure $\{p\}_t$ and the structural displacement $\{d\}_t$ are iterated simultaneously till a desired level of convergence is achieved. Thus, the iteration process is carried out till the conditions prescribed below are satisfied simultaneously

$$\left|\frac{\{p_{i+1}\}_t - \{p_i\}_t}{\{p_i\}_t}\right| \leq \varepsilon'', \quad \text{and} \quad \left|\frac{\{d_{i+1}\}_t - \{d_i\}_t}{\{d_i\}_t}\right| \leq \varepsilon'' \tag{B-2}$$

i being the number of iteration. ε'' is a small preassigned tolerance value. The most costly operation involved in the above algorithm is to successively solve two linear equation systems at each iteration. But in the present case, matrices involved in the solution of the system equations are decomposed into triangular forms at the beginning of the iteration, and thereby only two forward-eliminations and back-substitutions are required at each iteration step. Thus, the time required to obtain the coupled response for a particular time instant is minimized in the present iterative scheme.

References

[1] Ahmadi MT, Khoshrang G. Sefidrud dam's dynamic response to the large near-field earthquake of June 1990. Dam Eng 1992;3:85–113.
[2] Birk C, Ruge P. Representation of radiation damping in a dam–reservoir interaction analysis based on a rational stiffness approximation. Comput Struct 2007;85:1152–63.
[3] Bouaanani N, Paultre P, Proulx J. Two-dimensional modelling of ice-cover effects for dynamic analysis of concrete gravity dams. Earthquake Eng Struct Dyn 2002;31:2083–102.
[4] Bouaanani N, Paultre P, Proulx J. A closed-form formulation for earthquake-induced hydrodynamic pressure on gravity dams. J Sound Vib 2003;261:573–82.
[5] Chandrashaker R, Humar JL. Fluid–foundation interaction in the seismic response of gravity dams. Earthquake Eng Struct Dyn 1993;22:1067–84.
[6] Chavez JW, Fenves GL. Earthquake analysis of concrete gravity dams including base sliding. Earthquake Eng Struct Dyn 1995;24:673–86.
[7] Chopra AK. Earthquake behavior of reservoir–dam systems. J Eng Mech Div, ASCE 1968;93:1475–500.
[8] Chopra AK. Dynamics of structures. New Delhi: Prentice Hall of India Pvt. Ltd.; 1998, p. 155–85. ISBN-81-203-1043-8.
[9] Chopra AK, Chakrabarti P. The earthquake experience at Koyna dam and stresses in concrete gravity dams. Earthquake Eng Struct Dyn 1972;1:151–64.
[10] Chopra AK, Chakrabarti P. Earthquake analysis of concrete gravity dams including dam–water–foundation rock interaction. Earthquake Eng Struct Dyn 1981;9:363–83.
[11] Daniell WE, Mir RA, Simic MS, Taylor CA. Seismic behavior of concrete gravity dams. In 10th European conference on earthquake engineering, 28th August–2nd September, 1994, Vienna, Austria, A.A. Balkema, Rotterdam, 1995. p. 1951–1955.
[12] Darbre GR. Nonlinear reservoir–dam interaction by way of the hybrid frequency time procedure. In Proceedings of the 2nd European conference in structural dynamics, EURODYN'93, Trondhiem, Norway, A.A. Balkema, Rotterdam, 1993.
[13] El-Aidi B, Hall JF. Nonlinear earthquake response of concrete gravity dams. Earthquake Eng Struct Dyn 1989;187:837–65.
[14] Feltrin G, Galli M, Bachmann H. Influence of cracking on concrete gravity dams. In 10th world conference on earthquake engineering, AA Balkema, Rotterdam, Brookefield, 1992. p. 4627–32.
[15] Fenves G, Chopra AK. Earthquake analysis and response of concrete gravity dams. Report No.UCB/EERC-84/10, Earthquake Engineering Research Center, University of California, Berkley, California, 1984.
[16] Gabor D. Theory of communication. J Instit Elect Eng 1946;93(3):429–57.
[17] Gogoi I, Maity D. A non-reflecting boundary condition for the finite element modeling of infinite reservoir with layered sediment. Adv Water Resour 2006;29(10):1515–27.
[18] Gogoi I. Dynamic response of ageing concrete gravity dams with unbounded reservoir. PhD Thesis, I.I.T. Guwahati, 2006.
[19] Guan F, Moore ID, Lin G. Transient response of reservoir–dam–soil systems to earthquakes. Int J Numer Anal Meth Geomech 1994;18:863–80.
[20] Hall JF, Chopra AK. Two-dimensional dynamic analysis of concrete gravity and embankment dams including hydrodynamic effects. Earthquake Eng Struct Dyn 1982;10:305–32.
[21] Hatami K. Effect of reservoir bottom on earthquake response of concrete dams. Soil Dyn Earthquake Eng 1997;16:407–15.
[22] Haigh SK, Teymur B, Madabhushi SPG, Newland DE. Applications of wavelet analysis to the investigation of the dynamic behaviour of geotechnical structures. Soil Dyn Earthquake Eng 2002;22:995–1005.
[23] Humar JL, Roufaiel M. Finite element analysis of reservoir vibration. J Eng Mech 1983;109(1):215–30.
[24] Kotsubo S. Dynamic water pressure on dams during earthquake. In Second world conference on earthquake engineering, 1960. p. 799–814.
[25] Küçükarslan S. An exact truncation boundary condition for incompressible–unbounded infinite fluid domains. Appl Math Comput 2005;163(1):61–9.
[26] Li X, Romo MP, Avilés LJ. Finite element analysis of dam–reservoir systems using an exact far-boundary condition. Comput Struct 1996;60:751–62.
[27] Lotfi V. Analysis of response of dams to earthquakes, Geotechnical Engineering Report, GR86-2, Department of Civil Engineering, University of Texas, Austin, Texas, 1986.
[28] Maity D, Bhattacharya SK. Time domain analysis of infinite reservoir by finite element method using a novel far-boundary condition. Int J Finite Element Anal Design 1999;32:85–96.
[29] Nagarajaiah S, Varadarajan N. Short time Fourier transform algorithm for wind response control of buildings with variable stiffness TMD. Eng Struct 2005;27:431–41.
[30] Ruge P, Trinks C, Witte S. Time-domain analysis of unbounded media using mixed-variable formulations. Earthquake Eng Struct Dyn 2001;20:899–925.
[31] Safak E. Time-domain representation of frequency-dependent foundation impedance functions. Soil Dyn Earthquake Eng 2006;26:65–70.
[32] Saini SS, Bettess P, Zienkiewicz OC. Coupled hydrodynamic response of concrete gravity dams using finite and infinite elements. Earthquake Eng Struct Dyn 1978;6:363–74.
[33] Sharan SK. Finite element modelling of infinite reservoirs. J Eng Mech, ASCE 1985;111:1457–69.
[34] Sharan SK. A non-reflecting boundary in fluid–structure interaction. Computers and Structures 1987;26:841–6.
[35] Sharan SK. Efficient finite element analysis of hydrodynamic pressure on dams. Comput Struct 1992;42:713–23.
[36] Tsai CS, Lee GC. Method for transient analysis of threedimensional dam-reservoir interactions. J Eng Mech ASCE 1990;116:2151–72.
[37] Tsai CS, Lee GC, Ketter RL. A semi-analytical method for time-domain analysis of dam–reservoir interactions. Int J Numer Meth Eng 1990;29:913–33.
[38] Vargas-Loli LM, Fenves GL. Effects of concrete cracking on the earthquake response of gravity dams. Earthquake Eng Struct Dyn 1989;18:575–92.
[39] von Kármán T. Discussion of water pressures on dams during earthquakes. Trans ASCE 1933;98:434–6.
[40] Wepf DH, Wolf JP, Bachmann H. Hydrodynamic-stiffness matrix based on boundary elements for time domain dam–reservoir–soil analysis. Earthquake Eng Struct Dyn 1988;16:417–32.
[41] Westergaard HM. Water pressure on dams during earthquakes. Trans ASCE 1933;98:418–72.
[42] Wolf JP. Consistent lumped-parameter models for unbounded soil; frequency-independent stiffness, damping and mass matrices. Earthquake Eng Struct Dyn 1991;20:33–41.
[43] Wolf JP, Paronesso A. Lumped-parameter model of semi-infinite uniform fluid channel for time-domain analysis of dam–reservoir interaction. In Institut für Bodenmechanik und Felsmechanik, editor. Soil dynamics and earthquake engineering V. Germany: Universität Karlsruhe; 1991. p. 389–401.
[44] Zienkiewicz OC, Newton RE. Coupled vibration of a structure submerged in a compressible fluid. In Proceedings of international symposium on finite element techniques, Stuttgart, 1969.